Available online at www.sciencedirect.com

SCIENCE DIRECT®

Polymer 46 (2005) 12158–12165

polymer

www.elsevier.com/locate/polymer

# Syntheses and properties of electroluminescent polyfluorene-based conjugated polymers, containing oxadiazole and carbazole units as pendants, for LEDs

Youngeup Jin [a], Jin Young Kim [b], Sung Heum Park [b], Jinwoo Kim [a], Sungeun Lee [c], Kwanghee Lee [b], Hongsuk Suh [a,*]

[a] *Department of Chemistry and Center for Plastic Information System, Pusan National University, Pusan 609-735, South Korea*
[b] *Department of Physics, and Center for Plastic Information System, Pusan National University, Pusan 609-735, South Korea*
[c] *LG Electronics Institute of Technology, 16 Woomyeon-Dong, Seocho-Gu, Seoul 137-724, South Korea*

Received 4 July 2005; received in revised form 8 October 2005; accepted 18 October 2005
Available online 7 November 2005

## Abstract

New polyfluorenes (PF)-based conjugated copolymers, containing oxadiazole and carbazole units as pendants, were prepared as the electroluminescent (EL) layer in light-emitting diodes (LEDs) to show that most of them have higher maximum brightness and EL efficiency as compared to poly(2,7-(9,9-bis(2-ethylhexyl)fluorene)) (PF2/6). The prepared polymers, poly[(9-(6-(*N*-carbazolyl)-hexyl)-9-hexyl)-fluorene-2,7-diyl]-*co*-[(9-hexyl-9-(6-(4-(5-phenyl-1,3,4-oxadiazolyl)-phenoxy)-hexyl)-fluorene-2,7-diyl)] (Oxd-PF-*co*-Cz-PF), were soluble in common organic solvents and used as the EL layer in double layer light-emitting diodes (LEDs) (ITO/PEDOT/polymer/Al). All polymers show photoluminescence around $\lambda_{max}=430$ nm (exciting wavelength, 370 nm) and blue EL around $\lambda_{max}=426$ nm. The current–voltage–luminance (*I–V–L*) characteristics of the polymers show turn-on voltages of 3.5–5.5 V which are lower than that of PF2/6. The maximum brightness and EL efficiency of the device with the configuration of ITO/PEDOT/polymer/Al were 3000 cd/m$^2$ at 10 V and 2.13 cd/A at 10.6 mA/cm$^2$, respectively, which are all higher than those of PF2/6.

*Keywords:* Light emitting diode; Polyfluorene; Efficiency

## 1. Introduction

In the past few years polymer-based organic light-emitting diodes (OLEDs) have acquired much interests, and great efforts have been devoted to the design and synthesis of light-emitting polymers for practical applications [1–4]. There are a few appropriate polymers for fabricating OLEDs which emit green, orange, or red color [5–7]. A lot of attention has been paid to poly(9,9′-dialkylfluorene)s (PFs) as a prospective blue emitting layer for OLEDs [8–13]. PFs display high photoluminescence (PL) efficiencies both in solution and in solid films, with emission wavelengths primarily in the blue spectral region [14–17]. Photo-stability and thermal stability of PFs are also found to be better than those of the polyphenylenevinylenes (PPVs) [18]. PFs contain a rigid biphenyl unit, which leads to a large band gap with efficient blue emission, and the remote C-9 position, which allows facile substitution to improve the solubility, without significantly increasing the steric interaction with the polymer backbone.

Many of the conjugated polymers investigated as the light-emitting layer in OLEDs preferentially transport one of the injected charges. This generally results in an imbalance of charge transport and poor device efficiency. Many approaches have been taken to overcome the imbalance of charge carrier transport. The most frequent practices have been either to adjust the energy band of the polymer by introduction of electron-withdrawing groups as pendant groups or as part of the polymer backbone [19–21], or to use additional organic charge-transporting layers between the emissive layer and the electrodes [22]. Multi-layer device is utilizing hole-transport material (HTM) between anode and emitting layer, and electron-transport material (ETM) between emitting layer and cathode in order to improve the mobility of electron and hole. Tris(8-hydroxyquinoline)aluminum (Alq3), 2-(4-biphenylyl)-5-(4-*tert*-butylphenyl)-1,3,4-oxadiazole (PBD),

---

[*] Corresponding author. Tel.: +82 51 510 2203; fax: +82 51 516 7421.
*E-mail address:* hssuh@pusan.ac.kr (H. Suh).

0032-3861/$ - see front matter © 2005 Elsevier Ltd. All rights reserved.
doi:10.1016/j.polymer.2005.10.080

4,4′-bis(*N*-*m*-tolyl-*N*-phenylamino)biphenyl (TPD), and poly(*N*-vinylcarbazole) (PVK) have been used as the charge-transporting materials in LEDs [23,24]. In case of PBD, the electrons can pass through the PBD layer and easily reach the luminescent polymer, whereas the holes find a high barrier when they reach the polymer/PBD interface. This increases the probability that electrons and holes will meet and recombine, and the quantum efficiency is thereby increased. The multilayer device structure is composed of transparent anode/hole-transport layer (HTL)/emitting layer/electron-transport layer (ETL)/metal cathode. However, the multilayer device always result in an unfavorable increase in turn-on voltage and requires careful selection of material and solvent to avoid damage of emitting layer by spin-coating both HTL and ETL.

In the present work, we report the synthesis and electroluminescence properties of new EL polymer, [(9-hexyl-9-(6-(4-(5-phenyl-1,3,4-oxadiazolyl)-phenoxy)-hexyl)-fluorene-2,7-diyl)] (Oxd-PF), poly[(9-(6-(*N*-carbazolyl)-hexyl)-9-hexyl)-fluorene-2,7-diyl] (Cz-PF), and poly[(9-(6-(*N*-carbazolyl)-hexyl)-9-hexyl)-fluorene-2,7-diyl]-*co*-[(9-hexyl-9-(6-(4-(5-phenyl-1,3,4-oxadiazolyl)-phenoxy)-hexyl)-fluorene-2,7-diyl)] (Oxd-PF-*co*-Cz-PF) with carbazole and oxadiazole units as pendants in order to improve the charge carrier transport [25,26]. The electron-deficient moiety, 2,5-diphenyl-1,3,4-oxadiazole-diyl (Oxd), and the hole transporting moiety, *N*-carbazolyl (Cz), were introduced with flexible spacer of sufficient length as the side chain at the C-9 position of PF. The electrical and optical properties of Oxd-PF-*co*-Cz-PF samples were evaluated and compared with those of poly(2,7-(9,9-bis(2-ethylhexyl)fluorene) (PF2/6) which were synthesized using similar method as was used for the syntheses of other new polymers.

## 2. Experimental

Used all reagents were purchased from Aldrich or TCI, and used without further purification. Solvents were purified by normal procedure and handled under moisture-free atmosphere.

### 2.1. Instrumental characterization

$^1$H and $^{13}$C NMR spectra were recorded with a Varian Gemini-200 (200 MHz), Unityplus-300 (300 MHz) and Inova-500 (500 MHz) spectrometer and chemical shifts were recorded in ppm units with TMS as the internal standard. Flash column chromatography was performed with Merck silica gel 60 (particle size 230–400 mesh ASTM) with ethyl acetate/hexane or methanol/methylene chloride gradients unless otherwise indicated. Analytical thin layer chromatography (TLC) was conducted using Merck 0.25 mm silica gel 60F precoated aluminium plates with fluorescent indicator UV254. UV spectra were recorded with a Varian CARY-5E UV/vis spectrophotometer. The photoluminescence (PL) and electroluminescence (EL) spectra of the device were measured using an Oriel InstaSpec $\chi$ CCD detection systems. For PL spectrum measurements, xenon lamp was used as the excitation source, and incident beam took the maximum absorption peak of the polymers. Molecular weights and polydispersities of the polymers were determined by gel permeation chromatography (GPC) analysis with a polystyrene standard calibration. To examine electrochemical properties of the resulting polymer, the polymer film was cast from THF solution onto platinum plate as a working electrode with an area of 1 cm$^2$. Film thickness was controlled in the range of about 3 μm by the amount of solution. After coating, the film adhering to the electrode was dried in a vacuum oven for 10 h. The electrochemical measurements were performed on 0.1 M tetrabutylammonium tetrafluoroborate (TBAF, freshly distilled, Aldrich) solution in acetonitrile. A platinum wire and a Ag/AgNO$_3$ electrode were used as the counter electrode and reference electrode, respectively. Cyclic voltammetric waves were produced by using a EGandG Parc model 273 potentiostat/galvanostat at a constant scan rate of 100 mV/s.

### 2.2. EL device fabrication and measurements

For the EL experiment, poly(3,4-ethylenedioxythiophene) (PEDOT) doped with poly(styrenesulfonate) (PSS), as the hole-injection-transport layer, was introduced between emissive layer and ITO glass substrate cleaned by successive ultrasonic treatments. Isopropyl solution of the PEDOT/PSS was spin-coated on the surface-treated ITO substrate. On top of the PEDOT layer, the emissive polymer film was obtained by spin casting ODCB (*o*-dichlorobenzene) solution of the polymer. The emissive polymer thin film prepared had a uniform surface with a thickness of around 110 nm. The emissive film was dried in vacuum, and aluminum electrodes were deposited on the top of the polymer films through a mask by vacuum evaporation at pressures below $10^{-7}$ Torr, yielding active areas of 4 mm$^2$. For the determination of device characteristics, current–voltage (*I*–*V*) characteristics were measured using a Keithley 236 source measure unit. All processing steps and measurements mentioned above were carried out under air and at room temperature.

### 2.3. Synthesis of monomers

#### 2.3.1. 9-(6-Bromohexyl)-9*H*-carbazole (**2**)

To a stirred solution of NaH (60%) (2.9 g, 71.8 mmol) in THF (100 ml) at room temperature under argon was added 9*H*-carbazole (**1**) (10 g, 59.8 mmol) in THF (100 ml). After 10 min at room temperature, 1,6-dibromohexane (19 ml, 119.6 mmol) was added to the reaction mixture. After stirring overnight at reflux, the reaction mixture was treated with 200 ml of water. The aqueous layer was separated and extracted with 3× 100 ml methylene chloride. The combined organic layer was dried over MgSO$_4$, and concentrated in vacuo. The oily residue was purified by flash chromatography to give 12.68 g (64.2%) of 9-(6-bromohexyl)-9*H*-carbazole (**2**) as white solid [$R_f$: 0.30 (SiO$_2$, CH$_2$Cl$_2$/hexane = 1:4)]: $^1$H NMR (200 MHz, CDCl$_3$) $\delta$ (ppm): 1.39–1.55 (m, 4H), 1.74–1.96 (m, 4H), 3.36 (t, 2H, $J$ = 7.33 Hz), 4.31 (t, 2H, $J$ = 7.51 Hz), 7.21 (t, 2H, $J$ = 6.04 Hz), 7.27–7.52 (m, 4H), 8.10 (d, 2H, $J$ = 7.69 Hz): $^{13}$C NMR

(75 MHz, CDCl$_3$) $\delta$ (ppm): 26.30, 27.77, 28.67, 32.44, 33.63, 42.66, 108.51, 118.70, 120.25, 122.73, 125.52, 140.28.

### 2.3.2. *N′-Benzoyl-4-hydroxybenzohydrazide* (**4**)

A stirred solution of 4-hydroxy benzohydrazide (**3**) (10 g, 64.4 mmol) and benzoyl chloride (9.16 ml, 77.3 mmol) in 200 ml of pyridine was refluxed at 120 °C for 6 h under argon. After cooling to room temperature, 1 M HCl solution was added drop-wise for the acidification up to pH = 4–5. The mixture was poured into 500 ml of ethanol, and cooled to afford precipitation of 13.58 g (82.3%) of *N′*-benzoyl-4-hydroxybenzohydrazide (**4**) as white plate crystals: $^1$H NMR (200 MHz, DMSO) $\delta$ (ppm): 6.82 (d, 2H, $J=8.42$ Hz), 7.47–7.89 (m, 7H), 10.21 (s, 1H), 10.37 (s, 1H): $^{13}$C NMR (75 MHz, DMSO) $\delta$ (ppm): 122.85, 128.15, 129.20, 129.72, 129.76, 130.57, 132.55, 134.91, 165.81, 166.53.

### 2.3.3. *4-(5-Phenyl-1,3,4-oxadiazol-2-yl)phenol* (**5**)

A stirred solution of hydrazide compound **4** (13.5 g, 58.0 mmol) in SOCl$_2$ (200 ml) was refluxed at 80 °C for 5 h under argon. After excess SOCl$_2$ was distilled off, the residue was slowly poured into 500 ml of H$_2$O to give precipitation. After filtration, the filtrate was dried in vacuo for 12 h to give 10.3 g (74.7%) of 4-(5-phenyl-1,3,4-oxadiazol-2-yl)phenol (**5**): $^1$H NMR (200 MHz, DMSO) $\delta$ (ppm): 6.94 (d, 2H, $J=8.4$ Hz), 7.71–7.86 (m, 3H), 7.93 (d, 2H, $J=8.06$ Hz), 8.03–8.11 (m, 2H): $^{13}$C NMR (75 MHz, CDCl$_3$) $\delta$ (ppm): 122.65, 126.98, 128.41, 128.71, 129.11, 130.28, 131.80, 133.95.

### 2.3.4. *2-{4-[(6-Bromohexyl)oxy]phenyl}-5-phenyl-1,3,4-oxadiazole* (**6**)

To a stirred solution of NaH (60%) (1.23 g, 30.7 mmol) in THF (70 ml) at room temperature under argon was added oxadiazole compound **5** (6.1 g, 25.6 mmol) in THF (70 ml). After 10 min at room temperature, 1,6-dibromohexane (8.1 ml, 51.2 mmol) was added. After stirring overnight at reflux, the reaction mixture was treated with 200 ml of water. The aqueous layer was separated and extracted with $3\times100$ ml methylene chloride. The combined organic layer was dried over MgSO$_4$, and concentrated in vacuo. The oily residue was purified by flash chromatography to give 4.4 g (43.0%) of 2-{4-[(6-bromohexyl)oxy]phenyl}-5-phenyl-1,3,4-oxadiazole (**6**) as white solid [$R_f$: 0.40 (SiO$_2$, EA/hexane = 1:4)]: $^1$H NMR (200 MHz, CDCl$_3$) $\delta$ (ppm): 1.51–1.61 (m, 4H), 1.84–1.91(m, 4H), 3.43 (t, 2H, $J=6.78$ Hz), 4.04 (t, 2H, $J=6.23$ Hz), 7.01 (d, 2H, $J=8.43$ Hz), 7.51–7.55 (m, 3H), 8.06 (d, 2H, $J=9.16$ Hz), 8.10–8.15 (m, 2H): $^{13}$C NMR (75 MHz, CDCl$_3$) $\delta$ (ppm): 25.25, 27.88, 28.95, 32.63, 33.69, 67.99, 114.98, 116.32, 126.82, 128.33, 128.69, 129.02, 129.52, 131.49, 161.86.

### 2.3.5. *2,7-Dibromo-9-hexyl-9H-fluorene* (**8**)

To a stirred mixture of NaH (60%) (0.74 g, 18.5 mmol) in THF (50 ml) at room temperature under argon was added 2,7-dibromo-9*H*-fluorene (**7**) (5 g, 15.4 mmol) in THF (50 ml). After 10 min at room temperature, 1-bromohexane (2.16 ml, 15.4 mmol) was added. After stirring overnight at reflux, the reaction mixture was treated with 100 ml of water. The aqueous layer was separated and extracted with $3\times100$ ml methylene chloride. The combined organic layer was dried over MgSO$_4$, and concentrated in vacuo. The oily residue was purified by flash chromatography to give 2.74 g (43.6%) of 2,7-dibromo-9-hexyl-9*H*-fluorene (**8**) [$R_f$: 0.50 (SiO$_2$, hexane 100%)]: $^1$H NMR (500 MHz, DMSO-d$_6$) $\delta$ (ppm): 0.56 (br, 3H), 0.74–0.84 (m, 2H), 0.90–1.40 (m, 6H), 1.86–1.94 (m, 2H), 3.94 (br, 2H), 7.42–7.61 (m, 6H): $^{13}$C NMR (125 MHz, CDCl$_3$) $\delta$ (ppm): 14.35, 22.87, 23.70, 29.73, 31.73, 35.40, 36.91, 121.73, 122.37, 127.39, 132.86, 139.12, 146.65.

### 2.3.6. *2-(4-{[6-(2,7-Dibromo-9-hexyl-9H-fluoren-9-yl)hexyl]oxy}phenyl)-5-phenyl-1,3,4-oxadiazole* (**9**)

A solution of 2,7-dibromo-9-hexyl-9*H*-fluorene (**8**) (1.5 g, 3.67 mmol) and catalytic amounts of triethylbenzylammonium chloride in 30 ml of DMSO was stirred at 60 °C under argon. After 1 h at 60 °C, the reaction mixture was treated with bromide compound **6** (2.2 g, 5.5 mmol). After additional 1 h at 60 °C, the reaction mixture was treated with 20 ml of 50% aqueous NaOH at room temperature and stirred for 5 h. An excess amount of ethyl acetate was added to the reaction mixture to generate the precipitation of NaOH. After filtering off NaOH formed, the organic layer was washed with 100 ml of aqueous 1.0 M HCl solution, and 150 ml of H$_2$O. The organic layer was dried over MgSO$_4$ and concentrated in vacuo. The residue was purified by flash column chromatography to give 2.34 g (87.4%) of 2-(4-{[6-(2,7-dibromo-9-hexyl-9*H*-fluoren-9-yl)hexyl]oxy}phenyl)-5-phenyl-1,3,4-oxadiazole (**9**) [$R_f$: 0.30 (SiO$_2$, EA/hexane = 1:4)]: $^1$H NMR (300 MHz, DMSO-$d_6$) $\delta$ (ppm): 0.56–0.61 (m, 4H), 0.78 (t, 3H, $J=6.96$ Hz) 1.06–1.26 (m, 12H), 1.62–1.66 (m, 2H) 1.92 (t, 2H, $J=7.81$ Hz), 1.95 (t, 2H, $J=7.81$ Hz), 3.92 (t, 2H, $J=6.35$ Hz), 6.97 (d, 2H, $J=8.79$ Hz),), 7.45–7.54 (m, 9H), 8.03 (d, 2H, $J=8.79$ Hz), 8.12–8.14 (m, 2H): $^{13}$C NMR (75 MHz, CDCl$_3$) $\delta$ (ppm): 13.96, 22.54, 23.61, 25.61, 28.94, 29.53, 31.42, 36.21, 40.06, 40.20, 55.64, 68.07, 114.95, 116.18, 121.16, 121.50, 126.14, 126.82, 128.64, 129.01, 130.23, 131.47, 139.08, 152.40, 157.50.

### 2.3.7. *9-[6-(2,7-Dibromo-9-hexyl-9H-fluoren-9-yl)hexyl]-9H-carbazole* (**10**)

A solution of 2,7-dibromo-9-hexyl-9*H*-fluorene (**8**) (1.5 g, 3.67 mmol) and catalytic amounts of triethylbenzylammonium chloride in 30 ml of DMSO was stirred at 60 °C under argon atmosphere. After 1 h at 60 °C, to the reaction mixture was added bromide compound **2** (1.8 g, 5.5 mmol). After additional 1 h at 60 °C, the reaction mixture was treated with 20 ml of 50% aqueous NaOH solution at room temperature and stirred for 5 h. An excess amount of ethyl acetate was added to the reaction mixture to generate the precipitation of NaOH. After filtering off NaOH formed, the organic layer was washed with 100 ml of aqueous 1.0 M HCl solution, and 150 ml of H$_2$O. The organic layer was dried over MgSO$_4$ and concentrated in vacuo. The residue was purified by flash column chromatography to give 2.00 g (82.8%) of 9-[6-(2,7-dibromo-9-hexyl-9*H*-fluoren-9-yl)hexyl]-9*H*-carbazole (**10**) [$R_f$: 0.25 (SiO$_2$, CH$_2$Cl$_2$/hexane = 1:3)]: $^1$H NMR (500 MHz, CDCl$_3$) $\delta$ (ppm): 0.56–0.61 (m, 4H), 0.80 (t, 3H, $J=7.08$ Hz)

1.05–1.15 (m, 12H), 1.66–1.73 (m, 2H) 1.86–1.91 (m, 4H), 4.19 (t, 2H, $J=7.08$ Hz), 7.22 (t, 2H, $J=7.81$ Hz), 7.33 (d, 2H, $J=8.30$ Hz),), 7.42–7.53 (m, 8H), 8.10 (d, 2H, $J=7.81$ Hz): $^{13}$C NMR (75 MHz, $CDCl_3$) $\delta$ (ppm): 13.94, 22.52, 23.51, 23.56, 26.79, 28.74, 29.50, 29.58, 31.40, 39.96, 40.19, 42.83, 55.54, 108.57, 118.65, 120.27, 121.15, 121.47, 122.74, 125.53, 126.08, 130.20, 139.02, 140.33, 152.34.

### *2.4. Synthesis of polymers*

#### *2.4.1. Poly[(9-(6-(N-carbazolyl)-hexyl)-9-hexyl)-fluorene-2,7-diyl]-co-[(9-hexyl-9-(6-(4-(5-phenyl-1,3,4-oxadiazolyl)-phenoxy)-hexyl)-fluorene-2,7-diyl)] (Oxd-PF-co-Cz-PF), poly[(9-(6-(N-carbazolyl)-hexyl)-9-hexyl)-fluorene-2,7-diyl] (Cz-PF), poly[(9-hexyl-9-(6-(4-(5-phenyl-1,3,4-oxadiazolyl)-phenoxy)-hexyl)-fluorene-2,7-diyl)] (Oxd-PF) (**11**)*

The copolymers and homopolymers were synthesized by using monomers **9** and **10** of different ratio (10:0, 9:1, 7:3, 5:5, 3:7, 1:9, 0:10). In a two neck flask, were placed $Ni(COD)_2$ (393 mg, 1.43 mmol), 2,2′-dipyridyl (223 mg, 1.43 mmol), cyclooctadiene (0.175 ml, 1.43 mmol), and DMF (5 ml) by using Atmos Bag (Aldrich) under argon. The reaction mixture was heated at 80 °C for 0.5 h to form the purple complex. The monomers **9** and/or **10** (0.65 mmol) in toluene (6 ml) were added to the reaction mixture. After 3 days heating at 80 °C, 9-bromoanthracene (500 mg), the end capper, dissolved in 5 ml of anhydrous toluene was added to the reaction mixture. After heating at 80 °C for 24 h, the reaction mixture was cooled to room temperature, poured into the solution of 100 ml of aqueous 1.0 M HCl, 100 ml of acetone, and 100 ml of methanol. After stirring for 2 h, the solid were filtered, redissolved in THF, and recrystallized with large amount methanol. The precipitated polymer was filtered off, washed with water, and dried in vacuo at room temperature to afford the copolymers (Oxd-PF-*co*-Cz-PFs) and homopolymers (Oxd-PF and Cz-PF) **11** as white solid.

## 3. Results and discussion

### *3.1. Synthesis and characterization*

The general synthetic routes toward the monomers and polymers are outlined in Scheme 1. By using analogous methods as were reported, [27,28] 9-(6-bromohexyl)-9*H*-carbazole (**2**) and 2-{4-[(6-bromohexyl)oxy]phenyl}-5-phenyl-1,3,4-oxadiazole (**6**) were synthesized and coupled with mono alkylated 2,7-dibromo-9*H*-fluorene (**7**) to generate

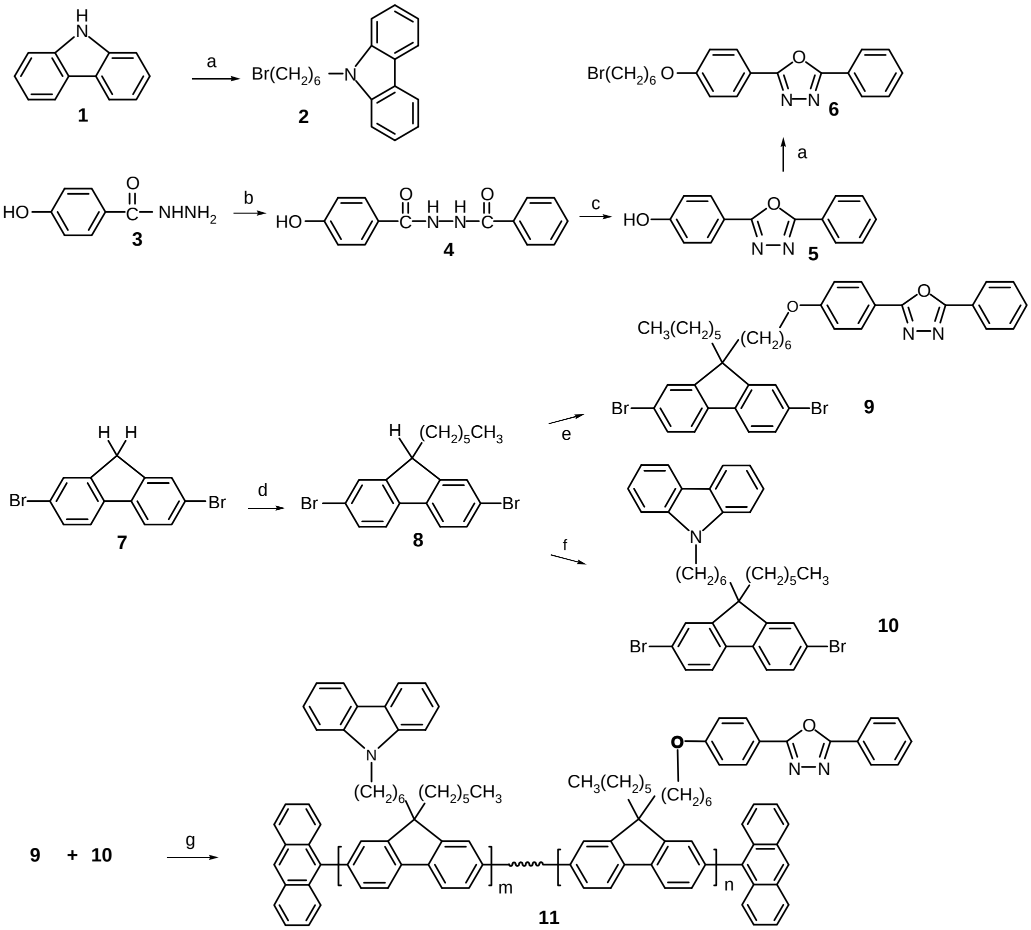

Scheme 1. Synthetic routes for the monomers and polymers: (a) NaH, $Br(CH_2)_6Br$, THF; (b) BzCl, pyridine; (c) $SOCl_2$; (d) NaH, $CH_3(CH_2)_5Br$, THF; (e) **6**, 50% aq. NaOH, triethylbenzylammonium chloride (TEBACl), DMSO; (f) **2**, 50% aq. NaOH, TEBACl, DMSO; (g) $Ni(COD)_2$, 2,2′-bipyridine, cyclooctadiene, 9-bromoanthracene, DMF/toluene.

Table 1
Polymerization results and thermal properties of the polymers

| Polymer | $M_n$[a] | $M_w$[a] | PDI[a] | $T_g$[b] (°C) | $T_d$[c] (°C) |
|---|---|---|---|---|---|
| Oxd-PF | 53,000 | 110,000 | 2.0 | 145 | 387 |
| Oxd-PF-*co*-Cz-PF (9:1) | 56,000 | 115,000 | 2.0 | 138 | 375 |
| Oxd-PF-*co*-Cz-PF (7:3) | 47,000 | 105,000 | 2.2 | 125 | 353 |
| Oxd-PF-*co*-Cz-PF (5:5) | 32,000 | 50,000 | 1.5 | 120 | 375 |
| Oxd-PF-*co*-Cz-PF (3:7) | 55,000 | 117,000 | 2.1 | 120 | 371 |
| Oxd-PF-*co*-Cz-PF (1:9) | 17,000 | 27,000 | 1.5 | 120 | 369 |
| Cz-PF | 40,000 | 90,000 | 2.2 | 122 | 384 |

[a] $M_n$, $M_w$, and PDI of the polymers were determined by gel permeation chromatography using polystyrene standards.
[b] $T_g$ were determined by DSC.
[c] $T_d$ were measured at a temperature of 5% weight loss for the polymers by TGA.

oxadiazole substituted monomer **9** and the carbazole substituted monomer **10**. The polymerizations for the copolymers containing these monomers of different ratios were generated under Yamamoto conditions [29] using Ni(0) catalysis to obtain Oxd-PF-*co*-Cz-PFs **11**. Homopolymers, Oxd-PF and Cz-PF, were also synthesized using the same condition. To be compared with the newly synthesized polymers, known poly(2,7-(9,9-bis(2-ethylhexyl)fluorene) (PF2/6) was synthesized using the analogous method.

The resulting Oxd-PF-*co*-Cz-PFs, Oxd-PF, and Cz-PF, brittle white polymers were soluble in organic solvents such as chloroform, chlorobenzene, THF, dichloromethane and ODCB. The emissive polymer films were obtained by spin-casting an ODCB solution of the polymers. The results of polymerization of Oxd-PF, Cz-PF, and Oxd-PF-*co*-Cz-PF are summarized in Table 1. The number-average molecular weight ($M_n$), weight-average molecular weight ($M_w$), and the polydispersities (PDI) of Oxd-PF-*co*-Cz-PF were in the range of 17,000–55,000, 27,000–117,000, and 1.5–2.2, respectively, as determined by GPC using THF as the eluant and polystyrene as the standard. The thermal properties of polymers were identified by TGA, and DSC thermograms. The weight losses of Oxd-PF, Cz-PF, and Oxd-PF-*co*-Cz-PF were less than 5% in heating to about 353–387 °C. The $T_g$ values for Oxd-PF, Cz-PF, and Oxd-PF-*co*-Cz-PF were observed to be 120–145 °C. The high $T_g$ values of present EL polymers prevent the deformation of polymer morphology and degradation of the polymeric emitting layer by applied electric fields of LEDs.

### 3.2. Optical and photoluminescence properties

The UV–vis absorption spectra and photoluminescence spectra of Oxd-PF-*co*-Cz-PFs with various compositions of Oxd-PF and Cz-PF as thin film are shown in Figs. 1 and 2. The thin films were prepared by spin-coating on quartz plates from the polymer solutions in ODCB. The absorption spectrum of the polymers exhibited three peaks at around 265, 300, and 390 nm, which are contributed to carbazole units, 1,3,4-oxadiazole units, and $\pi$–$\pi^*$ transition of the conjugated main chains, respectively. As the Oxd-PF content is increased, the absorption maximum peak of the carbazole units is decreased and the absorption maximum peak of the 1,3,4-oxadiazole is increased. The absorption onset wavelengths of all polymers were around 430 nm, which correspond to band gaps of 3.1 eV. Because all polymers have the same polyfluorene back-bone, the absorption spectra of these polymers were all similar. Fig. 2 shows emission spectra of the Oxd-PF-*co*-Cz-PFs thin films. The PL spectra of all polymer films consist of typical vibronically structured bands comprising a maximum, a shoulder, and a tail. The PL spectrum of all polymer films exhibits a maximum at around 430 nm, a shoulder at around 451 nm, and a tail at around 540 nm (exciting wavelength, 380 nm).

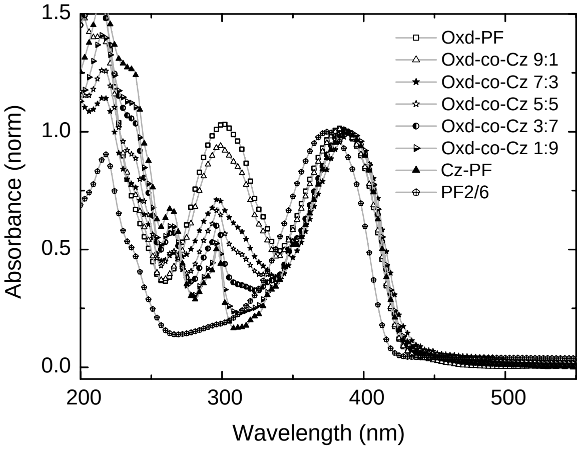

Fig. 1. UV–vis absorption spectra of the polymer films.

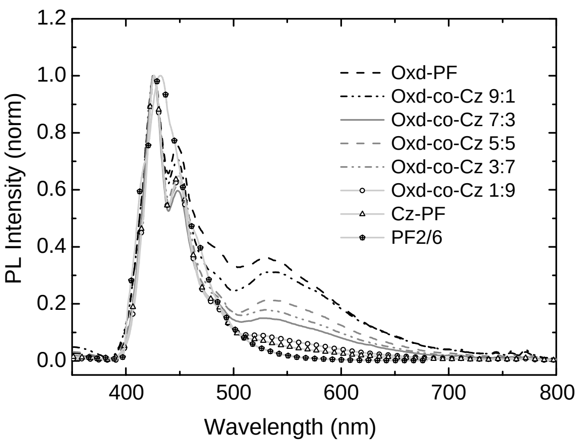

Fig. 2. PL emission spectra of the polymer films.

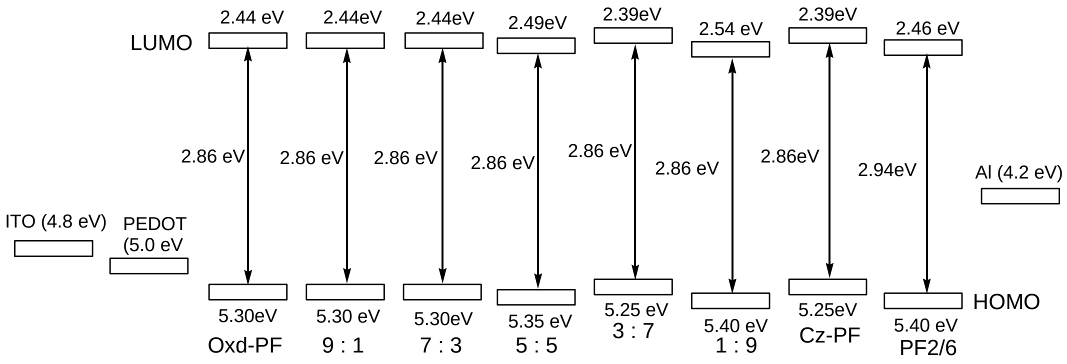

Fig. 3. Energy band diagram of polymers.

### *3.2.1. Electrochemical properties of the polymers*

The energy band diagrams, as shown in Fig. 3, of the polymers were determined from the band gaps which were estimated from the absorption edges, and the HOMO energy levels which were estimated from the cyclic voltammetry [30]. The CV was performed in a solution of tetrabutylammonium tetrafluoroborate ($Bu_4NBF_4$) (0.10 M) in acetonitrile at a scan rate of 100 mV/s at room temperature under argon atmosphere. A platinum electrode ($-0.05\ cm^2$) coated with a thin polymer film was used as the working electrode. A Pt wire and a $Ag/AgNO_3$ electrode were used as the counter electrode and reference electrode, respectively. All measurements were calibrated against an internal standard, ferrocene ($F_c$), which has the IP value ($-4.8$ eV) for the $F_c/F_c^+$ redox system [31]. Electrochemical properties of the polymers were measured to show that all of the polymers exhibit irreversible processes in an oxidation scan. The oxidation onsets of the polymers were estimated to be 0.80–0.95 V for Oxd-PF-*co*-Cz-PFs, which correspond to HOMO energy level of 5.25–5.40 eV. The LUMO energy levels of polymers were calculated with the HOMO and optical band gap. The LUMO energy levels of Cz-PF, Oxd-PF, and Cz-PF-*co*-Oxd-PFs were thus determined to be 2.39–2.54 eV. The electrochemical measurements reveal that the main chain determines their own electronic characteristics in the copolymer, although the electron-rich Cz and electron-deficient Oxd groups as pendants may lead to an increase in both hole and electron affinities and an improvement in charge injection of the polymer.

### *3.2.2. Electroluminescent properties and current–voltage–luminance*

The normalized electroluminescence spectra and the current–voltage characteristics of the ITO/PEDOT/polymers/Al device are shown in Figs. 4 and 5. To decrease the operating voltage and smooth the surface roughness of the indium tin oxide (ITO) electrode, the hole injection-transport layer, poly(3,4-ethylenedioxythiophene) doped with poly(styrenesulfonate) (PEDOT/PSS), was spin-coated from aqueous solution with isopropyl alcohol (10 wt%) on the surface-treated ITO substrate. On top of the PEDOT layer, the emissive polymer film was obtained by spin-casting an ODCB solution of the polymer. The emissive polymer thin film prepared had a uniform surface with a thickness of around 110 nm. The emissive film was dried in vacuum, and the aluminum electrode were deposited on the top of the polymer film through a mask by vacuum evaporation at pressure below about $10^{-6}$ mbar, yielding an active area of 4 $mm^2$.

Fig. 4 shows the EL spectra of ITO/PEDOT/polymer/Al devices. The EL spectra are similar to the PL spectra. The EL spectra of Oxd-PF-*co*-Cz-PFs exhibit maximum peaks at around 426 nm, which correspond to blue light. Because all polymers have the same polyfluorene back-bone, the EL spectra of these polymers were all similar. The same EL maximum peaks at around 426 nm is owing to the same effective conjugation length of the polymers. The difference of the ratios of Oxd-PF and Cz-PF does not affect the effective conjugation length of the polymers, since the oxadiazole and carbazole moieties were introduced as pendants using non-conjugated chain. All the copolymers and Oxd-PF showed an additional peak at around 540 nm. The origin of this low-energy emission band of various PF series, including aggregation and excimer formation in the material, is under investigation in many research groups. But it is interesting to see that Cz-PF homopolymer is showing almost no peak at around 540 nm. As shown in Fig. 6, this Cz-PF homopolymer showed the highest efficiency.

The current density–voltage and luminescence–voltage characteristics of ITO/PEDOT/polymers/Al devices are shown in Fig. 5. The current density–voltage characteristics

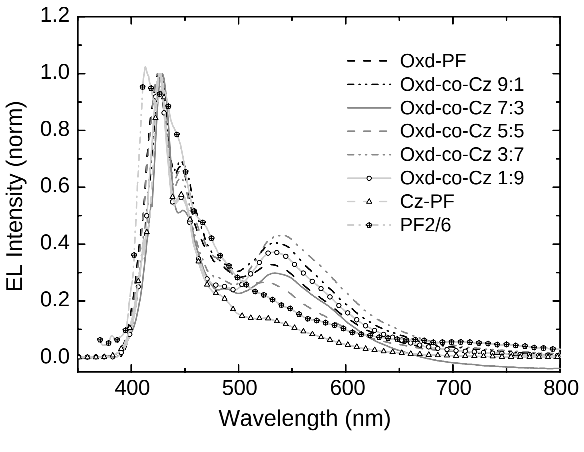

Fig. 4. EL spectra of the polymers with the configuration of ITO/PEDOT: PSS/polymer/Al.

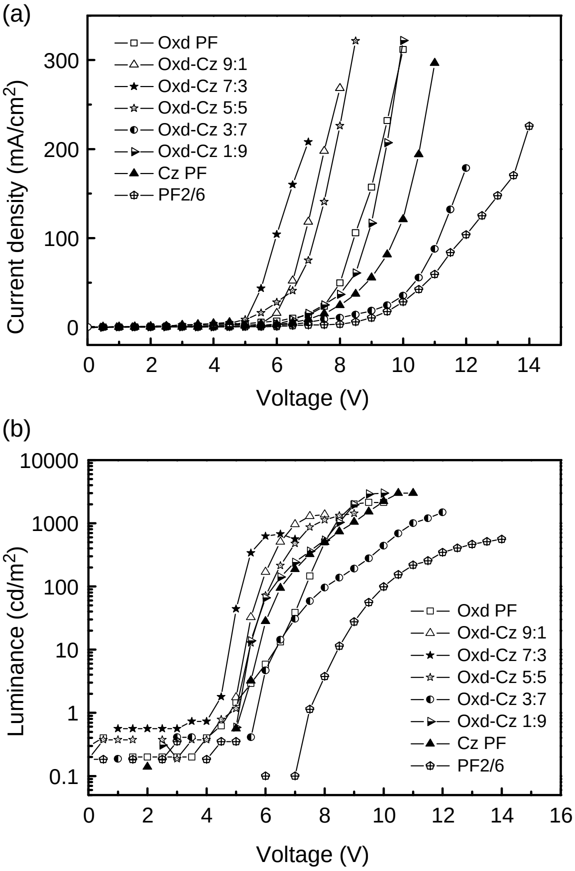

Fig. 5. (a) Current density–voltage (*J*–*V*), and (b) voltage–luminescence (*V*–*L*) characteristics of PLEDs of the polymers with the configuration of ITO/PEDOT:PSS/polymer/Al.

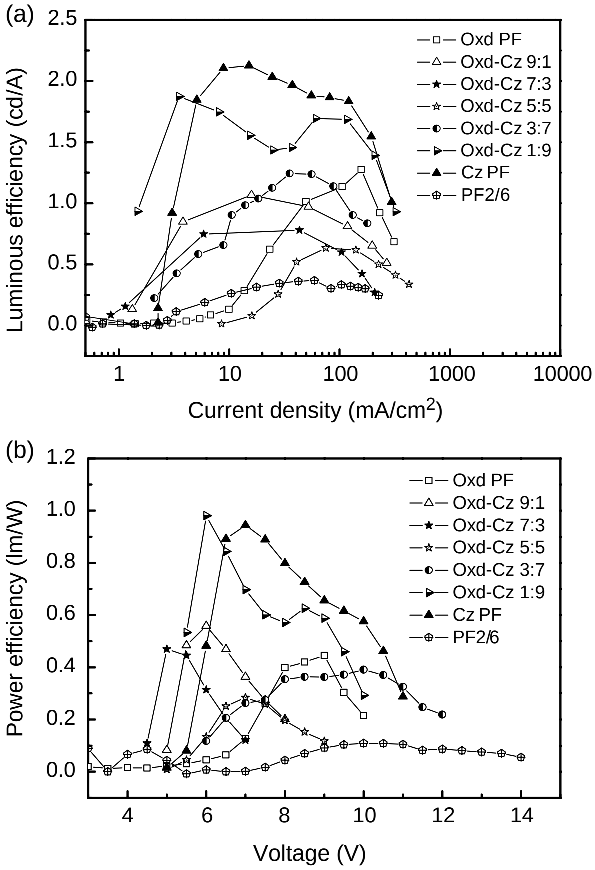

Fig. 6. Efficiency of PLEDs of the polymers with the configuration of ITO/PEDOT:PSS/polymer/Al (a) current density–efficiency (cd/A), and (b) voltage efficiency (1 m/W).

were measured using a Keithley 236 Source Measure Unit. All processing steps and measurements mentioned above were carried out under air and at room temperature. The turn-on voltage of ITO/PEDOT/polymers/Al devices are about 3.5–5.5 V which are all lower than that of PF2/6 (7 V). The luminescence intensities of the polymers are exponentially increased with an increase of voltage and higher than that of PF2/6. Especially, the maximum luminescence of Cz-PF and Oxd-PF-*co*-Cz-PF (1:9) with Al electrode are over 3000 cd/m$^2$ at 10 V.

Table 2 shows the 1931 Commission Internationale de L'Eclairage CIE coordinates of the PF derivatives. The CIE coordinates for the EL spectrum of Oxd-PF-*co*-Cz-PF (1:9) are (0.170, 0.089). With more amount of Oxd-PF unit in the copolymer, the x and y values of the CIE coordinates were increasing, which can be attributed to the $\pi$–$\pi^*$ aggregation caused by the 4-(5-phenyl-1,3,4-oxadiazol-2-yl)phenyl unit incorporated in the Oxd-PF unit.

All of the maximum EL efficiency of Oxd-PF, Cz-PF, and Oxd-PF-*co*-Cz-PFs (0.64–2.13 cd/A) are higher than that of PF2/6 (0.35 cd/A) as showed in Fig. 6. The maximum luminescence efficiency of Oxd-PF-*co*-Cz-PF (1:9) was 2.13 cd/A at 10.6 mA/cm$^2$. Especially, Cz-PF shows high maximum luminescence efficiency (1.85 cd/A) at low current density (3.8 mA/cm$^2$) as compared to PF2/6 (0.35 cd/A at 60.0 mA/cm$^2$). Oxadiazole and carbazole moieties, with flexible spacer of sufficient length as the side chain of the polymers, may provides a highly improved electron and hole transporting properties due to intra or inter chain interaction, which could be the reason of the lower turn-on voltages, and the higher maximum luminescences, and efficiencies as compared to PF2/6. It is under investigation in this laboratory to remove the low-energy emission band of PFs with the oxadiazole or carbazole moieties which are increasing efficiency and lowering the turn-on voltages.

Table 2
Device performance characteristics of the polymers

| Polymer | Turn-on (V) | LE$_{max}$[a] (cd/A) | CIE (*x*, *y*)[b] |
|---|---|---|---|
| Oxd-PF | 3.5 | 1.28 | (0.222, 0.211) |
| Oxd-PF-*co*-Cz-PF (9:1) | 4.3 | 1.06 | (0.243, 0.249) |
| Oxd-PF-*co*-Cz-PF (7:3) | 4.3 | 0.79 | (0.226, 0.213) |
| Oxd-PF-*co*-Cz-PF (5:5) | 4.5 | 0.64 | (0.217, 0.221) |
| Oxd-PF-*co*-Cz-PF (3:7) | 4.5 | 1.23 | (0.190, 0.120) |
| Oxd-PF-*co*-Cz-PF (1:9) | 5 | 1.89 | (0.170, 0.089) |
| Cz-PF | 5.5 | 2.13 | (0.184, 0.128) |

[a] Maximum luminescence.

[b] Calculated from the EL spectra.

## 4. Conclusion

In order to improve the charge carrier transport, we have synthesized, a new fully conjugated polymers, Oxd-PF, Cz-PF, and Oxd-PF-*co*-Cz-PFs containing polyfluorene backbone with pendants of carbazole moiety, and/or oxadiazole moiety by the Yamamoto polymerization. The electrochemical measurements reveal that the main chain determines their own electronic characteristics in the copolymer, although the electron-rich Cz and electron-deficient Oxd groups may lead to an increase in both hole and electron affinities and an improvement in charge injection of the polymers. The difference of the ratios of Oxd-PF and Cz-PF does not affect the effective conjugation length of the polymers, since the oxadiazole and carbazole moieties were introduced as pendants using non-conjugated chain. These carbazole and oxadiazole moieties may provide highly improved electron and hole transporting properties due to intra or inter chain interaction. These polymers have similar electrical and optical properties as compared to those of polyalkylfluorene (PF), and quite good thermal stability. The polymer LEDs of Oxd-PF, Cz-PF, and Oxd-PF-*co*-Cz-PFs emit EL maximum peak around 426 nm. The turn-on voltage of ITO/PEDOT/polymers/Al devices are about 3.5–5.5 V which are all lower than that of PF2/6 (7 V). The maximum luminescence of Cz-PF and Oxd-PF-*co*-Cz-PF (1:9) with Al electrode are over 3000 cd/m$^2$ at 10 V. All of the maximum EL efficiency of Oxd-PF, Cz-PF, and Oxd-PF-*co*-Cz-PFs (0.64–2.13 cd/A) are higher than that of PF2/6 (0.35 cd/A). The maximum luminescence efficiency of Oxd-PF-*co*-Cz-PF (1:9) was 2.13 cd/A at 10.6 mA/cm$^2$. Especially, Cz-PF shows high maximum luminescence efficiency (1.85 cd/A) at low current density (3.8 mA/cm$^2$) as compared to PF2/6 (0.35 cd/A at 60.0 mA/cm$^2$). The CIE coordinates of the EL spectrum of Oxd-PF-*co*-Cz-PF (Oxd 1:Cz 9) are (0.170, 0.089), which are quite close to that of the standard blue (0.140, 0.080) of NTSC. Especially, in case of Cz-PF, the peak at around 540 nm was not observed but the polymer showed highest efficiency.

## Acknowledgements

This work was supported by Korean Research Foundation Grant (KRF-2003-002-C00145) (H. Suh).

## References

[1] Friend RH, Gymer RW, Holmes AB, Burroughes JH, Marks RN, Taliani C, et al. Nature 1999;397:121.
[2] Kraft A, Grimsdale AC, Holmes AB. Angew Chem, Int Ed 1998;37:402.
[3] Jin Y, Kim J, Lee S, Kim JY, Park SH, Lee K, et al. Macromolecules 2004;37:6711.
[4] Kim TH, Park JH, Lee TW, Park OO. Polymer 2004;45:8567.
[5] Burroughes JH, Bradley DDC, Brown AR, Marks RN, Mackay K, Friend RH, et al. Nature 1990;347:539.
[6] Braun D, Heeger AJ. Appl Phys Lett 1991;58:1982.
[7] Greenham NC, Moratti SC, Bradley DDC, Friend RH, Holmes AB. Nature 1993;365:628.
[8] Charas A, Morgado J, Martinho JMG, Alcacer L, Lim SF, Friend RH, et al. Polymer 2003;44:1843.
[9] Mikroyannidis JA, Beka PM, Papadopoulos JF. Synth Met 2005;149:203.
[10] Pei Q, Yang Y. J Am Chem Soc 1996;118:7416.
[11] Cirpan A, Ding L, Karasz FE. Polymer 2005;46:811.
[12] Ranger M, Rondeau D, Leclerc M. Macromolecules 1997;30:7686.
[13] Grell M, Bradley DDC, Inbasekaran M, Woo EP. Adv Mater 1997;9:798.
[14] Klaerner G, Miller RD. Macromolecules 1998;31:2007.
[15] Kreyenschmidt M, Klaerner G, Fuhrer T, Ashenhurst J, Karg S, Chen WD, et al. Macromolecules 1998;31:1099.
[16] Grice AW, Bradley DDC, Bernius MT, Inbasekaran M, Wu WW, Woo EP. Appl Phys Lett 1998;73:629.
[17] Janietz S, Bradley DDC, Grell M, Giebeler C, Inbasekaran M, Woo EP. Appl Phys Lett 1998;73:2453.
[18] Leclerc M. J Polym Sci, Part A: Polym Chem 2001;39:2870.
[19] Jang MS, Song SY, Shim HK. Polymer 2000;41:5675.
[20] Jin Y, Ju J, Kim J, Lee S, Kim JY, Park SH, et al. Macromolecules 2003;36:6970.
[21] Boardman FH, Grice AW, Ruther MG, Sheldon TJ, Bradley DDC, Burn PL. Macromolecules 1999;32:111.
[22] Burn PL, Grice AW, Tajbakhsh A, Bradley DDC, Thomas AC. Adv Mater 1997;9:1171.
[23] Lee YZ, Chen SA. Synth Met 1999;105:185.
[24] Winkler B, Meghdadi F, Tasch S, Evers B, Schneider I, Fischer W, et al. Synth Met 1999;102:1083.
[25] Lee YZ, Chen X, Chen SA, Wei PK, Fann WS. J Am Chem Soc 2001;123:2296.
[26] Kang HS, Kim KH, Kim MS, Park KT, Kim KM, Lee TH, et al. Synth Met 2002;130:279.
[27] Li X, Wang J, Mason R, Bu XR, Harrison J. Tetrahedron 2002;58:3747.
[28] Zhan X, Liu Y, Wu X, Wang S, Zhu D. Macromolecules 2002;35:2529.
[29] Klärner G, Lee JI, Lee VY, Chan E, Chen JP, Nelson A, et al. Chem Mater 1999;11:1800.
[30] Pommerehne J, Vestweber H, Guss W, Mahrt RF, Bässler H, Porsch M, et al. Adv Mater 1995;7:551.
[31] de Leeuw DM, Simenon MMJ, Brown AR, Einerhand REF. Synth Met 1997;87:53.